J|A|C|S
ARTICLES
Published on Web 05/05/2006

A Low-Temperature Synthesis for Organically Soluble HgTe Nanocrystals Exhibiting Near-Infrared Photoluminescence and Quantum Confinement

Marc-Oliver M. Piepenbrock, Tom Stirner, Stephen M. Kelly,* and Mary O'Neill*

Contribution from the Departments of Chemistry and Physics, University of Hull, Hull HU6 7RX, United Kingdom

Received January 31, 2006; E-mail: s.m.kelly@hull.ac.uk; m.oneill@hull.ac.uk

Abstract: A new low-temperature, one-pot method is introduced for the preparation of organically passivated HgTe nanocrystals, without the use of highly toxic precursors. The nanocrystals show bright photoluminescence in the infrared telecommunication windows about 1300 and 1550 nm with quantum efficiencies between 55 and 60%. They have a zinc blende structure with a mean particle diameter of 3.4 nm, thus exhibiting quantum confinement effects. Particle growth is self-limited by temperature quenching, so a narrow size distribution is obtained. The measured size of the particles agrees with calculations using the pseudopotential method.

Over the past decade the preparation and characterization of semiconductor nanocrystals (NCs) has met with increasing interest.[1−4] These colloidal quantum dots (QDs), as they are also referred to, show potential for applications in diverse fields ranging from LEDs,[5] lasers,[6] and solar cells[7] to bio-organic tagging.[8] Any preparation method has to produce monodisperse and highly crystalline quantum dots in order to fulfill this potential. In general, this is achieved either by synthesis in an aqueous medium[9] or via an organometallic route.[10] The latter method provides a relatively simple way for the preparation of organically soluble II−VI semiconductor NCs capped by tri-*n*-octylphosphine oxide (TOPO) and is now used to prepare various semiconducting QDs.[11,12]

While II−VI semiconductor NCs such as CdSe have been prepared routinely and extensively studied, the synthesis of mercury chalcogenide QDs still remains a challenge. Of these chalcogenides, HgTe is of interest for applications in the optoelectronics industry, since its emission covers the low-loss transmission windows in silica telecommunication fibers, which lie at around 1300 nm (0.95 eV) and 1550 nm (0.79 eV).[13] HgTe NCs stabilized by 1-thiolglycerol have been successfully prepared by aqueous methods.[14] However, an additional ligand-exchange step has to be undertaken to produce organically soluble QDs, which are required for spin-coating processes used in LED fabrication.[15] This can lead to a decrease in the PL efficiency and a shift in the PL emission maximum.[16] Brennan et al. were the first to investigate an organometallic approach to the preparation of HgTe.[17] They reported fast growth and flocculation of the particles to bulk HgTe on exposure to room lights. Green et al.[18] used a modification of the early tri-*n*-octylphosphine (TOP/TOPO) method[10] to grow large organically passivated NCs of HgTe along with some bulk material. The particles did not show quantum confinement properties nor any detectable PL. Unlike other II−VI semiconductors that require high temperatures (120−300 °C) for the growth of high-quality NCs, the growth was too rapid even at the relatively low temperature of 70 °C because of the ionic nature of HgTe. Here we show that temperature quenching rather than heating gives high quality crystalline NCs. We report for the first time a one-pot organometallic preparation of organically soluble HgTe nanoparticles with a spherical shape, narrow size dispersity and a high PL quantum yield in the near-IR telecommunication windows.

(1) Weller, H. *Angew. Chem., Int. Edit. Engl.* **1993**, *32* (1), 41−53.
(2) Alivisatos, A. P. *J. Phys. Chem.* **1996**, *100* (31), 13226−13239.
(3) Eychmüller, A. *J. Phys. Chem. B* **2000**, *104* (28), 6514−6528.
(4) Kelly, S. M.; O'Neill, M.; Stirner, T. *Handbook of Electroluminescent Materials*; Vij, D. R., Ed.; IoP Publishing: Bristol, 2004; Chapter 4, pp 158−192.
(5) Colvin, V. L.; Schlamp, M. C.; Alivisatos, A. P. *Nature* **1994**, *370* (6488), 354−357.
(6) Klimov, V. I.; Mikhailovsky, A. A.; Xu, S.; Malko, A.; Hollingsworth, J. A.; Leatherdale, C. A.; Eisler, H. J.; Bawendi, M. G. *Science* **2000**, *290* (5490), 314−317.
(7) Greenham, N. C.; Peng, X. G.; Alivisatos, A. P. *Synth. Met.* **1997**, *84* (1−3), 545−546.
(8) Gaponik, N.; Radtchenko, I. L.; Sukhorukov, G. B.; Weller, H.; Rogach, A. L. *Adv. Mater.* **2002**, *14* (12), 879−882.
(9) Rogach, A. L.; Katsikas, L.; Kornowski, A.; Su, D. S.; Eychmüller, A.; Weller, H. *Ber. Bunsen-Ges. Phys. Chem.* **1996**, *100* (11), 1772−1778.
(10) Murray, C. B.; Norris, D. J.; Bawendi, M. *J. Am. Chem. Soc.* **1993**, *115* (19), 8706−8715.
(11) Peng, Z. A.; Peng, X. G. *J. Am. Chem. Soc.* **2001**, *123* (1), 183−184.
(12) Trindade, T.; O'Brien, P.; Pickett, N. L. *Chem. Mater.* **2001**, *13* (11), 3843−3858.
(13) Harrison, M. T.; Kershaw, S. V.; Burt, M. G.; Rogach, A. L.; Kornowski, A.; Eychmüller, A.; Weller, H. *Pure Appl. Chem.* **2000**, *72* (1−2), 295−307.
(14) Harrison, M. T.; Kershaw, S. V.; Burt, M. G.; Rogach, A. L.; Kornowski, A.; Eychmüller, A.; Weller, H. *Mater. Res. Soc. Symp. Proc.* **1999**, *536*, 217−222.
(15) Koktysh, D. S.; Gaponik, N.; Reufer, M.; Crewett, J.; Scherf, U.; Eychmüller, A.; Lupton, J. M.; Rogach, A. L.; Feldmann, J. *ChemPhysChem* **2004**, *5* (9), 1435−1438.
(16) Gaponik, N.; Talapin, D. V.; Rogach, A. L.; Eychmüller, A.; Weller, H. *Nano Lett.* **2002**, *2* (8), 803−806.
(17) Brennan, J. G.; Siegrist, T.; Carroll, P. J.; Stuczynski, S. M.; Reynders, P.; Brus, L. E.; Steigerwald, M. L. *Chem. Mater.* **1990**, *2* (4), 403−409.
(18) Green, M.; Wakefield, G.; Dobson, P. J. *J. Mater. Chem.* **2003**, *13* (5), 1076−1078.

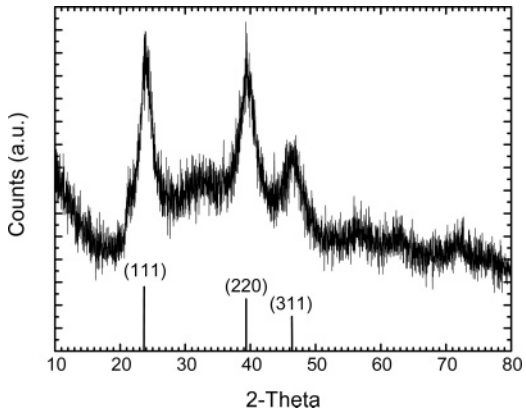

Figure 1. Powder X-ray diffraction pattern of HgTe nanoparticles freshly isolated as a dry powder. Also shown are the reflections from zinc blende bulk HgTe (coloradoite).

In a typical synthesis mercury(II) acetate (0.33 g, 1.0 mmol) was dissolved in ethanol (15 mL). Hexadecylamine (1.00 g, 4.2 mmol) was added to the reaction solution and after dissolving immediately formed a white precipitate on reaction with the mercury precursor. This precipitate went into solution upon gently heating the reaction mixture to 50 °C with vigorous stirring under nitrogen flow. Once a clear solution had formed, it was cooled by immersion of the flask in dry ice. During the cooling a TOPTe complex, formed by dissolving tellurium powder (0.13 g, 1.0 mmol) in TOP (2 mL), was slowly added dropwise to the mercury precursor solution. The solution slowly turned brown and eventually a precipitate was formed, typically on addition of 0.3 mL of the TOPTe solution, as the mixture reached a sufficiently low temperature. At this stage no more tellurium precursor was added. The mixture was then allowed to cool completely and left at −78 °C for about 10 min until it had solidified. Samples from the mixture were taken and dissolved in toluene for further investigation. The crystals were precipitated by washing the cold reaction mixture with ethanol (50 mL). The precipitate was collected by centrifugation, washed again with acetone (50 mL), isolated by a second centrifugation, and dried under vacuum. The final product took the form of a dark brown powder, which could be dissolved readily in toluene.

The reaction of mercury(II) acetate with TOPTe in cold ethanol as described above resulted in the formation of nanosized zinc blende HgTe. The particles are crystalline, as determined by powder X-ray diffraction (XRD) measurements shown in Figure 1. The wide-angle peaks indicate the zinc blende phase and correspond to diffractions from the 111, 220, and 311 planes of bulk HgTe coloradoite. The angular positions of the peaks are the same as those obtained by Harrison et al. for HgTe prepared in water.[14] The peaks are broadened compared to those of bulk HgTe, indicating the small particle size. The mean size of the particles is estimated to be 3.2 nm in diameter from the full width at half-maximum of the 111 reflection using the Scherrer equation (assuming a shape parameter of 0.9) and are therefore similar in size to those produced by aqueous methods. It is remarkable, given the normal growth temperatures for NCs, that good quality crystals are obtained at the low temperatures used in this synthesis. Electron microscopy of the HgTe QDs (Figure 2) shows almost spherical particles with a mean diameter of 3.5 nm and a size variation of about ±10%. The average particle size is in good agreement with the value from powder XRD. The particle sizes are very small compared to previous

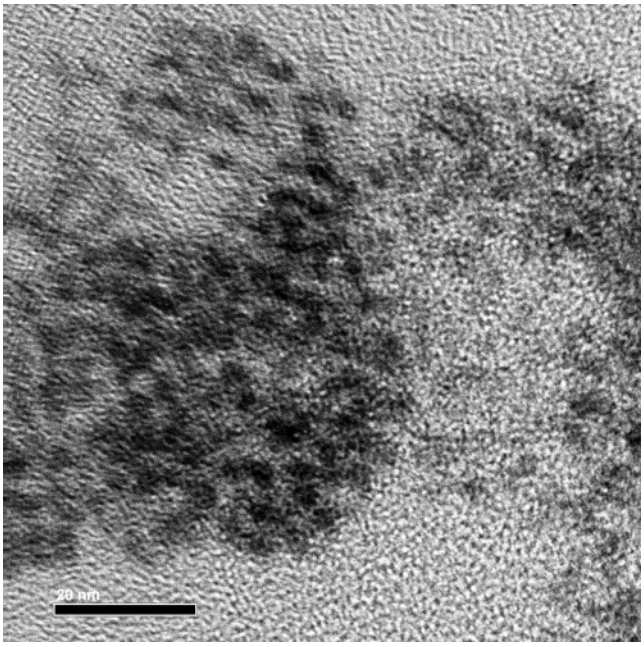

Figure 2. The TEM image of HgTe QDs freshly isolated as described in the text and redissolved in toluene shows roughly spherical particles. The scale bar represents 20 nm.

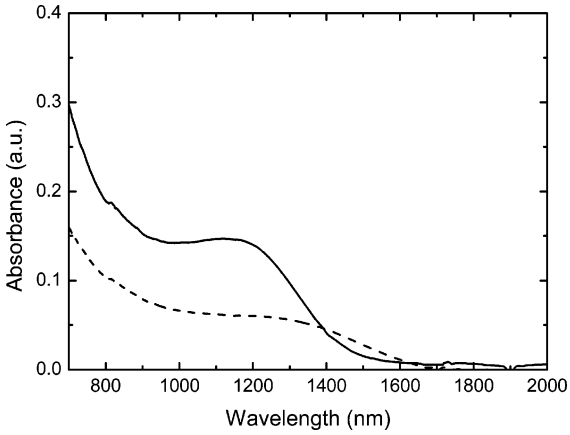

Figure 3. Absorption spectra of HgTe nanoparticles prepared as described in the text. The more pronounced peak at 1120 nm (full line) belongs to the freshly prepared particles, and the one at 1290 nm (dashed line) belongs to a sample after 2 weeks of aging.

organometallic preparations, highlighting the importance of a low-temperature reaction. The chemical composition of the HgTe NCs was determined by ICP measurements. The ratio of Hg:Te was found to be 1.4:1, meaning the crystals are mercury-rich. CdSe QDs prepared by organometallic routes showed similar deviation from the expected Cd:Se ratio of 1:1, which was attributed to nonstoichiometric, cadmium-rich surface layers.[19]

The absorption spectra of HgTe crystals dispersed in toluene were taken immediately after preparation and subsequently after 2 weeks of aging in the toluene solvent. Typical results are shown in Figure 3. Bulk HgTe has a small negative band-gap at room temperature, so the observation of a well-defined absorption peak from the freshly prepared sample at 1120 nm confirms quantum confinement. After 2 weeks the peak is

(19) Taylor, J.; Kippeny, T.; Rosenthal, S. J. *J. Clust. Sci.* **2001**, *12* (4), 571−582.

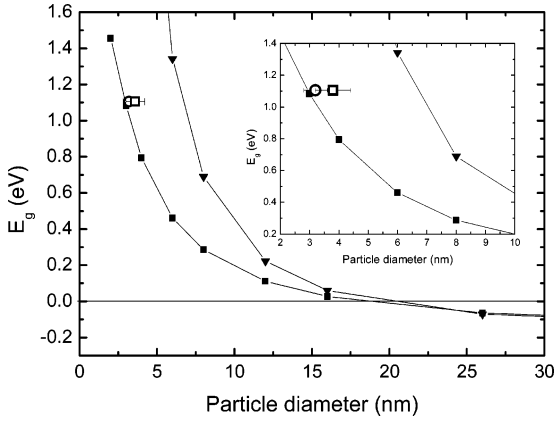

Figure 4. Calculated band gap versus diameter for HgTe QDs using the pseudopotential method (squares) and effective mass theory (triangles). For the pseudopotential calculation the semimetal-to-semiconductor transitions is predicted to occur at $D \approx 18$ nm. The open circle and open square give the diameter of QDs calculated from X-ray data and TEM images. The lines on the calculated graphs are a guide to the eye only. The inset shows the same information on a different spatial scale.

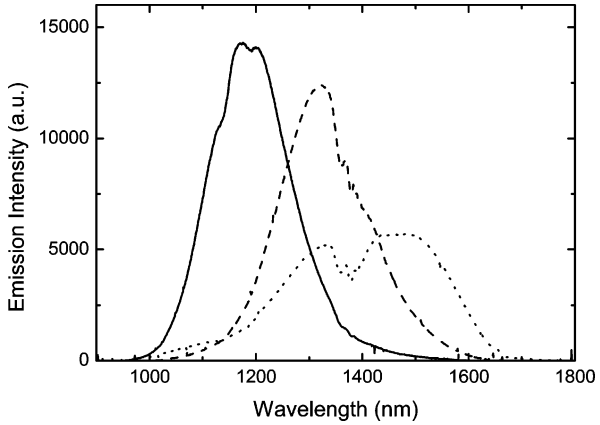

Figure 5. PL spectra of HgTe QDs taken for freshly prepared (solid line), 2-day-old (dashed line), and 2-week-old (dotted line) nanocrystals in toluene. All samples were excited with a HeNe laser at 632.8 nm.

broadened with a red shift to ∼1290 nm. No significant further shift is observed after even longer aging time periods. This aging effect will be discussed below. The absorption peaks can be used to estimate the size of the HgTe NCs via comparison with the calculations of the variation of band-gap with particle size. The effective mass approximation was previously used for HgTe NCs,[18] but it breaks down when the particle diameter is small. The pseudopotential calculation includes nonparabolic dispersion of the band-edge states and has been previously used by us to calculate the radii of CdTe QDs.[20,21] Both calculations are limited by the assumption of an infinite potential and closer agreement with experimental results would be expected if the actual confinement of the electrons and holes were considered. This is not possible without a free parameter, since the band offsets between the conduction and valence bands of the semiconductor and the LUMO and HOMO energies of the stabilizer and solvent are unknown. The closed square data points of Figure 4 show the band-gap energy as a function of HgTe NC diameter obtained using pseudopotential calculations, assuming spherical particles. Published zinc blende HgTe pseudopotential form factors were used,[22] and the spin−orbit interaction was modeled as previously described.[23] On the basis of these calculations we can estimate the particle diameter from the first absorption peak at 1120 nm (=1.105 eV) to be 3.0 nm, which, as Figure 4 shows, agrees well with the results obtained from powder XRD and TEM. The band energy is also calculated using the effective mass approximation. The results are shown as closed triangles in Figure 4 and predict a diameter of 6.7 nm for a corresponding absorption peak of 1120 nm, which does not agree with structural measurements. Hence, the pseudopotential calculation provides a much more accurate estimation of the particle size, especially for smaller diameters. Using the pseudopotential calculation a size distribution of ±20% is obtained from the spectral width of the exciton absorption feature of the NCs.

In contrast with previous attempts to synthesize organically passivated HgTe QDs,[17,18] the nanoparticles prepared by our method show strong luminescence in the range between 1200 and 1600 nm, thus covering the 1.3 and 1.55 μm windows, which are important for telecommunication applications. PL emission spectra, shown in Figure 5, were taken from samples dissolved in toluene, excited by a HeNe laser (632.8 nm). Freshly prepared HgTe nanoparticles show strong PL emission with a peak maximum at ∼1200 nm. The quantum efficiency (QE) of the HgTe nanocrystals was estimated using a comparative method as previously used for CdSe and CdTe QDs.[26] The dye Pyridine 2 was used as the standard and had a QE of ∼15% as measured using an integrating sphere.[27] Freshly prepared HgTe NCs show a quantum efficiency between 55 and 60%, which compares well with the best results achieved for thiol-stabilized HgTe.[13,14] Aging is observed after 2 days when the particles are left in solution and stored in the dark in air. The peak shifts to a wavelength of 1320 nm. Samples that were isolated and washed with ethanol and then redispersed in toluene show similar behavior when kept in solution for a similar time period. The aging of the particles was monitored over 8 weeks, but after aging for approximately 2 weeks, the PL spectrum remains constant over time. Noting that the trough in the 2-week-old PL spectrum at ∼1400 nm is due to a transmittance minimum of toluene at this wavelength, the aged PL spectrum covers both the infrared telecommunication fiber transmission windows at 1.3 and 1.55 μm.[16] The quantum efficiency maintains a relatively high value of ∼26% after 2 weeks. The red shift and broadening of both absorption and PL spectra during the aging process suggest a colloidal growth process. In particular, the red-shift of the PL maximum, the broadening of the absorption and emission lines, and the asymmetry of the latter spectrum for aged samples appear to be consistent with the defocusing of the particle size distribution predicted by recent Monte Carlo simulations of Ostwald ripening.[24,25] A similar aging effect was also observed for thiol-stabilized water-soluble HgTe particles.[13] However, for the present method it is

(20) Stirner, T.; Kirkman, N. T.; May, L.; Ellis, C.; Nicholls, J. E.; Kelly, S. M.; O'Neill, M.; Hogg, J. H. C. *J. Nanosci. Nanotechnol.* **2001**, *1* (4), 451−455.
(21) Stirner, T. *J. Chem. Phys.* **2002**, *117* (14), 6715−6720.
(22) Bouarissa, N. *Infrared Phys. Technol.* **1998**, *39* (5), 265−270.
(23) Bloom, S.; Bergstresser, T. K. *Solid State Commun.* **1968**, *6* (7), 465−467.
(24) De Smet, Y.; Deriemaeker, L.; Finsy, R. *Langmuir* **1997**, *13* (26), 6884−6888.
(25) Talapin, D. V.; Rogach, A. L.; Shevchenko, E. V.; Kornowski, A.; Haase, M.; Weller, H. *J. Am. Chem. Soc.* **2002**, *124* (20), 5782−5790.
(26) Jose, R.; Biju, V.; Kamakoa, Y.; Nagase, T.; Makita, Y.; Shinohara, Y.; Baba, Y.; Ishikawa, M. *Appl. Phys. A* **2004**, *79* (8), 1833−1838.
(27) de Mello, J. C.; Wittmann, H. F.; Friend, R. H. *Adv. Mater.* **1997**, *9* (3), 230−232.

remarkable that the particles keep growing to a saturated limit at room temperature in toluene even after they have been isolated and stored as a powder. Taking the absorption peaks for fresh and aged particles and calculating the size by the pseudopotential method give a change in the particle diameter of approximately 0.5 nm. The band energies of NCs are sensitive to their environment, so an alternative explanation for the spectral changes on aging may be a surface modification of the NCs in solution, which changes the potential energy of the NC environment. The loss in QE during the aging process may indicate a small degree of oxidation, leading to the formation of surface trap states, which in turn quench the photoluminescence.

Unlike the aqueous growth method, which gives a broad distribution of particles sizes, particle growth is self-limiting by temperature quenching so that only a narrow distribution ($\leq \pm 20\%$) is obtained. The synthesis is highly reproducible with variations in the absorption peak of only ± 30 nm over several samples. The current procedure gives NCs that emit in the important telecommunications windows, but different particles sizes may be obtained by initiating growth at higher temperatures or by adding larger quantities of TOPTe to the cadmium precursor solution.

In conclusion, a new and simple low-temperature approach to organically passivated HgTe QDs is presented. The particles exhibit strong PL, which covers the IR range between 1200 and 1600 nm with QEs between 55 and 60%. This property makes the particles potentially interesting for telecommunication applications, e.g., optical amplification or hybrid inorganic−organic light-emitting diodes (HIOLEDs). The present one-pot synthesis produces organically soluble NCs that show quantum confinement effects and a highly crystalline zinc blende structure. The diameter of the particles was estimated from powder X-ray diffraction data and TEM images and found to lie in the range of 3.4 ± 0.3 nm. The experimental results were found to be incompatible with effective-mass theory, assuming infinite potentials. However, they are in good agreement with theoretical calculations using the pseudopotential method assuming infinite potentials, thereby demonstrating the importance of effects such as band nonparabolicity in the simulations.

Acknowledgment. We thank Gordon Sowersby for technical support. Jan Halder is also acknowledged for TEM images, Bob Knight for ICP results, Andy Wilson for X-ray powder diffraction data, and Khue T. Lai for absorption measurements. We thank the EPSRC for funding the research.

JA060721J